Universal Dimer in a Collisionally Opaque Medium: Experimental Observables and Efimov Resonances

Olga Machtey, David A. Kessler, and Lev Khaykovich[*]

Department of Physics, Bar-Ilan University, Ramat-Gan, 52900 Israel
(Received 24 November 2011; published 30 March 2012)

A universal dimer is subject to secondary collisions with atoms when formed in a cloud of ultracold atoms via three-body recombination. We show that in a collisionally opaque medium, the value of the scattering length that results in the maximum number of secondary collisions may not correspond to the Efimov resonance at the atom-dimer threshold and thus cannot be automatically associated with it. This result explains a number of controversies in recent experimental results on universal three-body states and supports the emerging evidence for the significant finite range corrections to the first excited Efimov energy level.

Few-body systems with a resonantly enhanced two-body scattering length a display universal properties in the sense that they are independent of the details of the short-range interaction potential [1]. In the two-body domain with repulsive interactions, the most weakly bound energy level of the universal dimer depends solely on a, scaling as $1/a^2$. The central paradigm in the three-body domain, predicted in the early 1970s by Efimov [2], is associated with the infinite ladder of universal bound states with discrete scaling invariance. Beside a, universal trimers depend on the three-body parameter, which accounts for all the short-range physics not already included in a. In recent experiments with ultracold atoms many aspects of universality were verified mainly by localizing Efimov resonances which are associated with the crossing points of the trimers' binding energy levels with either the three-atom (for $a < 0$) or the atom-dimer (for $a > 0$) continua (for a recent review see Ref. [3]). Surprisingly, positions of the lowest Efimov resonances for $a < 0$ were found to be universally related to the van der Waals lengths of the two-body interaction potentials in different atomic species [4–14] indicating a universal three-body parameter. This remarkable experimental discovery has attracted intense theoretical attention which suggests a whole new understanding of Efimov physics in ultracold atoms [15,16]. However, the situation with the Efimov resonances at the atom-dimer threshold (for $a > 0$) remains unclear. It appears to significantly deviate from the universal picture in all species investigated to date [6,9,13,17–20]. Suggestions have been made that the finite range of interaction potentials might be responsible for these discrepancies. However, here we show that in some cases a different effect, directly related to the specifics of the experimental observables, can cause a significant shift in the resonances' positions.

To show this effect we start by elaborating on two experimental strategies developed recently to localize an Efimov resonance at the atom-dimer threshold, denoted in the following as a_*. Both are based on the theoretical prediction that resonant enhancements of the atom-dimer elastic (σ_e) and inelastic (σ_i) cross sections are expected in the vicinity of a_*, according to the following analytical expressions [1,21]:

$$\sigma_e = 84.9 \frac{\sin^2[s_0 \ln(a/a_*) + 0.97] + \sinh^2 \eta_*}{\sin^2[s_0 \ln(a/a_*)] + \sinh^2 \eta_*} a^2, \quad (1)$$

$$\sigma_i = \frac{20.3}{3v} \frac{\sinh(2\eta_*)}{\sin^2[s_0 \ln(a/a_*)] + \sinh^2 \eta_*} \frac{\hbar a}{m_A}, \quad (2)$$

where $s_0 = 1.00624$, η_* is the lifetime of the Efimov state, v is the velocity of the dimer and m_A is the mass of the atom [22]. In the first strategy, realized with ultracold Cs and ^{6}Li, an atom-dimer mixture is initially prepared in a shallow optical trap and the decay rate of dimers is then monitored as a function of a [13,17–19]. Thus, in this approach, the maximum of the enhancement in the atom-dimer *inelastic* collision rate is expected to coincide with a_*. In the second strategy, pioneered with ^{39}K [6] and then used with ^{7}Li [9,24], the three-body recombination induced loss rate of atoms is measured. In each recombination event a universal dimer is formed with initial kinetic energy equal to one third of its binding energy ($E_d/3$), which is usually much higher than the shallow optical trap depth. Moreover, the dimer is formed with the largest probability at the trap center where the density is highest. Then, on its way out, it may undergo secondary collisions with atoms, eject them out of the trap and cause the number of lost atoms per recombination event to greatly exceed three. Therefore, in this approach, the position of the maximum of the atom-dimer *elastic* collision rate is anticipated to reveal a_*.

In this Letter we consider the problem of secondary collisions of dimers with atoms and develop a model to calculate their mean number as a function of a. Our central message is that the elastic and the inelastic processes are intimately interrelated and cannot be considered

independently. According to Eqs. (1) and (2), σ_i and σ_e are both enhanced when $a = a_*$, however variations in σ_e may exceed those of σ_i by orders of magnitude which impacts the experimental observables in a nontrivial way. Applying this model to the experimental results of Refs. [6,9,24], we show that main controversies in the second experimental approach can be resolved when these processes are correctly included. We clarify the Efimov resonance' positions in ^{7}Li and ^{39}K and support the emerging evidence for significant finite range corrections to the first excited Efimov energy level in both systems [24].

In the following we assume that the number of dimers is always very small compared to the number of trapped atoms and thus we neglect collisions between them. This situation is correct for all the experimental realizations considered here. We start with presenting two possible scenarios that a dimer can undergo on its way out of the trap: (i) The dimer collides elastically with k atoms and leaves the trap due to a high enough kinetic energy. (ii) After k elastic collisions, the dimer undergoes one inelastic collision, decays to a deeper bound state and leaves the trap without any further scattering events because σ_e and σ_i are enhanced only for the weakly bound universal dimers. To evaluate the probabilities of each scenario, we divide the total length l of the dimers' journey through the atomic cloud into N segments of infinitesimally small length δl. Then, most generally, the probability to have an elastic or inelastic collision in the length segment δl is: $p_{e/i} = \sigma_{e/i}\bar{n}\delta l$, where $\bar{n}$ is the mean density of atoms [25]. Consequently, the probability to have no events in the same segment is $p_{\text{none}} = 1 - p_i - p_e$.

According to Eq. (2), σ_i depends on velocity and thus changes at each elastic collision because the dimer transfers a part of its initial kinetic energy to an atom. However, it is instructive to start with the assumption that σ_i remains constant independent of energy which makes the model clearer and analytically more tractable. Moreover, this simplification is reasonable in the limit of few collisional events and high initial energies of the dimer. Experimentally it is realized in the region of relatively small scattering lengths and moderate atom densities which corresponds to some of the experimental conditions considered later on.

Energy independent (analytical) model.

Scenario (i): The probability for k elastic events to occur can be expressed by the choice of k segments out of total N, $\binom{N}{k}$, in which the elastic scatterings occur with the probability p_e^k and multiplying it by the probability p_{none}^{N-k} that in the remaining $(N-k)$ segments no events happen. This probability is given by

$$p_{k,0} = \binom{N}{k} p_e^k p_{\text{none}}^{N-k} \xrightarrow[\delta l \to 0]{} P(k; \sigma_e \bar{n}l) \exp(-\sigma_i \bar{n}l), \quad (3)$$

where $P(k; x)$ is the Poisson distribution. Note that although an inelastic event is not involved in scenario i,

the probability $p_{k,0}$ does depend on σ_i. This is because the probability of no inelastic event has to be included as a factor.

Scenario (ii): The inelastic event, which happens after k elastic collisions, has to occur at any of the $N-k$ last segments with the probability p_i. First, we fix the inelastic event at the mth place where $m \in [k+1, N]$. Then, the procedure is similar to that of scenario i. The probability for k elastic collisions to occur is expressed by the choice of k segments out of total $m-1$, $\binom{m-1}{k}$, with the probability p_e^k multiplied by the probability p_{none}^{m-1-k} that in the remaining $m-1-k$ segments no scattering events occur. Thus, the total probability for scenario ii is just the sum over all possible locations of m:

$$p_{k,1} = \sum_{m=k+1}^{N} \binom{m-1}{k} p_{\text{none}}^{m-1-k} p_e^k p_i \xrightarrow[\delta l \to 0]{} \int_0^l \frac{(\sigma_e \bar{n}x)^k}{k!}$$
$$\times \exp[-(\sigma_e + \sigma_i)\bar{n}x]\sigma_i \bar{n} dx. \quad (4)$$

The mean number of scattering events in each scenario is then evaluated as the sum of weighted probabilities [27]:

$$\bar{N}_{e,0} = \sum_{k=1}^{\infty} k p_{k,0} = \sigma_e \bar{n}l \exp(-\sigma_i \bar{n}l), \quad (5)$$

$$\bar{N}_{e,i} = \sum_{k=0}^{\infty} (k+1) p_{k,1} = [1 - \exp(-\sigma_i \bar{n}l)]$$
$$+ \frac{\sigma_e}{\sigma_i}[1 - \exp(-\sigma_i \bar{n}l)(1 + \sigma_i \bar{n}l)]. \quad (6)$$

Finally, the total mean number of events is then $\bar{N} = \bar{N}_{e,0} + \bar{N}_{e,i}$. The central result of the Letter is already seen in Eqs. (5) and (6): both of them include the interplay between elastic and inelastic cross sections which strongly affects the experimental observables.

Energy dependent model.—Now we revamp the model taking into account the energy dependence of σ_i. When a dimer is created via a three-body recombination, its energy is significantly larger than the kinetic energy of atoms. The mean energy of the dimer is reduced by a factor of $1/\alpha^2 = 5/9$ per elastic collision with a nearly stationary atom [28]. As before, we calculate the probabilities and the mean number of events for each scenario.

Scenario (i): Let us consider k elastic events. Then the first one can occur only at any of the first $N - (k-1)$ segments with the probability p_e. We fix its location at the segment j_1 leaving the remaining $j_1 - 1$ segments to have no scattering events with the probability $(1 - p_i\alpha^0 - p_e)^{j_1-1}$. Next, we fix the second scattering position j_2 which then can only occur between segments $j_1 + 1$ and $N - (k-2)$ with the probability p_e. In the remaining $(j_2 - 1) - j_1$ segments no events happen with the probability $(1 - p_i\alpha^1 - p_e)^{j_2-j_1-1}$ and so on until the location j_k is fixed. Finally, the total probability of k elastic events is evaluated by the sum of all these cases:

$$p_{k,0} = p_e^k \sum_{j_1=1}^{N-k+1} \sum_{j_2=j_1+1}^{N-k+2} \cdots \sum_{j_k=j_{k-1}+1}^{N} \prod_{m=1}^{k}(1 - p_i\alpha^{m-1} - p_e)^{j_m - j_{m-1} - 1}(1 - p_i\alpha^k - p_e)^{N-k}, \quad \text{where } j_0 = 0. \quad (7)$$

Scenario (ii): Here the probability is constructed almost identically to that of scenario i, but with one variation. Before counting the elastic events we fix the segment where a single inelastic event occurs at the mth position where $m \in [k + 1, N]$. As a result, elastic events can happen only in the first $m - 1$ segments and we count them as in scenario i. Thus, the total probability for scenario ii is just the sum over all possible locations of m:

$$p_{k,1} = p_e^k p_i \sum_{m=k+1}^{N} \sum_{j_1=1}^{m-k} \sum_{j_2=j_1+1}^{m-k+1} \cdots \sum_{j_k=j_{k-1}+1}^{m-1} \prod_{s=1}^{k}(1 - p_i\alpha^{s-1} - p_e)^{j_s - j_{s-1} - 1}(1 - p_i\alpha^k - p_e)^{m-k-1}\alpha^k, \quad (8)$$

where $j_0 = 0$. In the limit of $\delta l \to 0$, Eqs. (7) and (8) take the form

$$p_{k,0} = \left(\frac{\sigma_e}{\sigma_i}\right)^k \sum_{j=0}^{k} \frac{\exp[-(\sigma_i\alpha^j + \sigma_e)\bar{n}l]}{\prod_{m=0, m \neq j}^{k}(\alpha^m - \alpha^j)}, \quad (9)$$

$$p_{k,1} = \left(\frac{\sigma_e}{\sigma_i}\alpha\right)^k \sum_{j=0}^{k} \frac{1 - \exp[-(\sigma_e + \sigma_i\alpha^j)\bar{n}l]}{(\frac{\sigma_e}{\sigma_i} + \alpha^j)\prod_{m=0, m \neq j}^{k}(\alpha^m - \alpha^j)}, \quad (10)$$

which reduce to Eqs. (3) and (4) as $\alpha \to 1$. The mean number of events $\bar{N}(a)$ can now be evaluated numerically based on the sum of weighted probabilities [see Eqs. (5) and (6)]. We now turn to apply the model to the recent experimental results which use the second experimental strategy.

^{7}Li: Ref. [9] reports $a_* = 608a_0$, which should be corrected to $a_* \sim 410a_0$ due to the shift in position of the Feshbach resonance [8,23]. However, recent measurement of Machtey *et al* (MSGK) [24], based on the same experimental technique reveals $a_* = 196(4)a_0$ which is away from the Rice result by many times the experimental uncertainty. There is, however, a major difference in the experimental conditions used by the two groups: while MSGK work with a low density thermal gas [8,24], the Rice experiment is performed on a Bose-Einstein condensate (BEC). According to Ref. [9], the mean density of atoms in the BEC is $\bar{n} \approx 5 \times 10^{12}$ cm^{-3} and half of the geometrical mean of the Thomas-Fermi radius is $l \approx 160$ μm. In the MSGK case, for a typical temperature of $T = 1.4$ μK, radial and longitudinal trap frequencies of $\omega_r = 2\pi \times 1.3$ kHz and $\omega_z = 2\pi \times 190$ Hz and $\sim 3.5 \times 10^4$ atoms, the mean atom density is $\bar{n} \approx 1 \times 10^{12}$ cm^{-3}. The geometrical mean size of the atomic cloud is $l \approx 9.5$ μm (1 standard deviation of the Gaussian distribution). Therefore the column density ($\bar{n}l$) in the Rice experiment is larger by a factor of ~ 80.

For the second strategy, all scenarios contribute to the experimental observable and so we show $\bar{N}(a)$ in Fig. 1 for both experiments. We used the energy dependent model with $a_* = 196a_0$. The solid red (dashed-dotted blue) line corresponds to the MSGK (Rice) experimental conditions. In the MSGK case, the maximum in $\bar{N}$ nearly perfectly

coincides with the position of a_*, which indicates that the experimental observable indeed reveals the position of the Efimov resonance. However, for the Rice experimental parameters, the maximum of $\bar{N}$ is not at a_* but rather appears at $\sim 375a_0$, in very good agreement with the reported result [9]. A simple intuitive understanding of this difference can be obtained when the limit of $\sigma_i\bar{n}l \ll 1 (\gg 1)$, roughly matching MSGK (Rice) experimental conditions, is taken in Eqs. (5) and (6). Then in the MSGK case, $\bar{N} \approx \sigma_e\bar{n}l$, which corresponds to the mean number of the elastic collisions and peaks at the maximum of σ_e, i.e., at $a = a_*$. However, for the Rice case, $\bar{N} \approx 1 + \sigma_e/\sigma_i$, which is maximized at a different position, namely, when $s_0 \ln(a/a_*) + 0.97 = \pi/2$ [see Eqs. (1) and (2)] [29]. This corresponds to $a/a_* \approx 1.8$ in agreement with the energy dependent model and the Rice result.

Note that the model predicts a larger width of the $\bar{N}(a)$ maximum for the Rice experimental conditions, qualitatively well identified in the experimental results [9,24] and, thus, further strengthening our model. However, quantitative comparison requires inclusion of additional conditions such as reduction of the dimer energy below the trap depth after a certain number of elastic collisions. Here we only associate the maximum in the three-body recombination loss rate with the maximum in the mean number of secondary collisions. In the region of large a not all of them, if
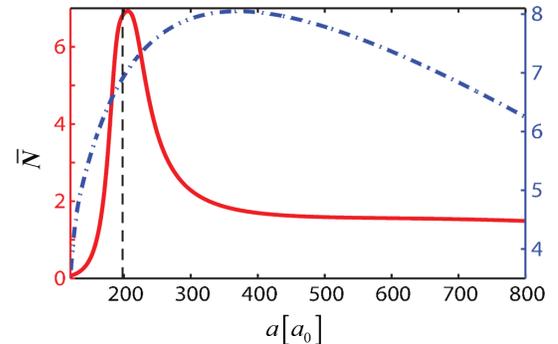

FIG. 1 (color online). $\bar{N}(a)$ for the experimental parameters of Ref. [8] (solid red line) and Ref. [9] (dashed-dotted line). Parameters of the Efimov resonance are $a_* = 196a_0$ (marked with the dashed vertical line) and $\eta_* = 0.1$.
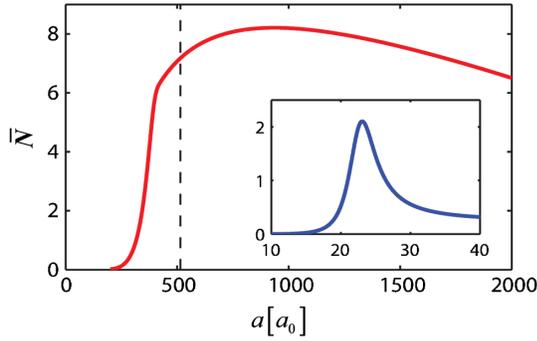
FIG. 2 (color online). $\bar{N}(a)$ for the experimental parameters of Ref. [6]. Inset shows a peak at low scattering length which also reasonably agrees with the experiment. Parameters of the Efimov resonance are $a_* = 515a_0$ (marked with the dashed vertical line) and $\eta_* = 0.1$.

any, lead to atom loss, which cuts down the long tail of $\bar{N}(a)$. This is, however, beyond the scope of the present discussion.

^{39}K: In Ref. [6] two Efimov resonances at the atom-dimer threshold are reported at $a_{*1} = 30.4a_0$ and $a_{*2} = 930a_0$. We shall concentrate our analysis on the second resonance as the first one is deeply inside the nonuniversal region where $a_{*1} < r_0$ with $r_0 = 64.5a_0$ being the van der Waals length of ^{39}K. The experiment is also performed in a BEC with $\bar{n} \approx 6.5 \times 10^{12}$ cm^{-3} and half of the geometrical mean of the Thomas-Fermi radius is $l \approx 7$ μm. As before our model predicts a significant shift in the real position of the resonance as compared to the reported one. To agree with the experimental value of $\sim 930a_0$ we need to take $a_* = 515a_0$, which reflects the same numerical factor of 1.8 as before. $\bar{N}(a)$ is shown in Fig. 2. In the inset we represent the second peak located at $\sim 23a_0$ and calculated with the slightly different experimental parameters in accordance to Ref. [6] but with the same a_*. Although it is close to the measured value it might be merely a coincidence. Note also the difference in widths of the two features which again qualitatively agrees with the experiment.

We can now compare the newly extracted positions of the Efimov resonances at the atom-dimer threshold for both species with the values predicted by universal theory (see Table I). In both cases a_* is notably shifted to lower values. MSGK associate this shift with the manifestation of finite range corrections [24,30]. For ^{7}Li the shift is smaller than for ^{39}K. In both cases the Feshbach resonances are of intermediate character between being closed and open channel dominated, but r_0 of ^{7}Li is about half that of ^{39}K. It is interesting to note that in Cs the shift is even larger despite the open channel dominated character of the Feshbach resonance (see Table I) [4,17,18]. However, the r_0 of Cs is the largest among the other species and we can then conclude that the recent experimental results support a scaling of the finite range corrections in r_0. Finally, we note

TABLE I. Comparison between newly extracted values of the Efimov resonances at the atom-dimer threshold (a_*) and the values predicted by universal theory (a_*^{UT}). While a_*^M denotes the originally reported experimental results, a_* shows the corrected values of a_*^M according to our model if applicable. a_0^* indicates positions of recombination minima in the measured three-body recombination spectra and is used to find a_*^{UT} via a universal relation $a_*^{UT} \approx 1.1a_0^*(22.7)^{n-1/2}$ where n can be either 0 or 1 for the purpose of this Table.

	$a_0^*[a_0]$	$a_*^{UT}[a_0]$	$a_*^M[a_0]$	$a_*[a_0]$	a_*^{UT}/a_*	$r_0[a_0]$
^{7}Li [24]	1260^a	291	196	$=a_*^M$	1.48	32.5
^{7}Li [9]^b	$\sim$1288	$\sim$297	$\sim$410	$\sim$220	$\sim$1.4	32.5
^{39}K [6]	224	1174	930	515	2.28	64.5
^{39}K [6]	5650	1305	930	515	2.53	64.5
^{133}Cs [18]	210^c	1100	397	$=a_*^M$	2.77	101

^{a}See also Ref. [8].
^{b}The values are rescaled according to correct Feshbach resonance parameters, i.e., position and energy width [8,23].
^{c}See also Refs. [4,5]. Note that a_0^* is reasonably well related to an Efimov resonance at $a < 0$ [4] despite the fact that it is too close to r_0 and thus might be subject to the finite range corrections.

that experiments provide growing evidence for a good agreement of the position of the lowest minimum in the three-body recombination spectrum with universal theory despite the fact that it is measured at even lower scattering lengths than a_* [4–6], which still remains a puzzling question.

This work was supported, in part, by the Israel Science Foundation.

*lev.khaykovich@biu.ac.il
[1] E. Braaten and H.-W. Hammer, Phys. Rep. **428**, 259 (2006).
[2] V. Efimov, Phys. Lett. B **33**, 563 (1970).
[3] F. Ferlaino, A. Zenesini, M. Berninger, B. Huang, H.-C. Nägerl, and R. Grimm, Few-Body Syst. **51**, 113 (2011).
[4] T. Kraemer, M. Mark, P. Waldburger, J. G. Danzl, C. Chin, B. Engeser, A. D. Lange, K. Pilch, A. Jaakkola, H.-C. Nägerl, and R. Grimm, Nature (London) **440**, 315 (2006).
[5] M. Berninger, A. Zenesini, B. Huang, W. Harm, H.-C. Nägerl, F. Ferlaino, R. Grimm, P. S. Julienne, and J. M. Hutson, Phys. Rev. Lett. **107**, 120401 (2011).
[6] M. Zaccanti, B. Deissler, C. D'Errico, M. Fattori, M. Jona-Lasinio, S. Müller, G. Roati, M. Inguscio, and G. Modugno, Nature Phys. **5**, 586 (2009).
[7] N. Gross, Z. Shotan, S. Kokkelmans, and L. Khaykovich, Phys. Rev. Lett. **103**, 163202 (2009).
[8] N. Gross, Z. Shotan, S. Kokkelmans, and L. Khaykovich, Phys. Rev. Lett. **105**, 103203 (2010).
[9] S. E. Pollack, D. Dries, and R. G. Hulet, Science **326**, 1683 (2009).
[10] T. B. Ottenstein, T. Lompe, M. Kohnen, A. N. Wenz, and S. Jochim, Phys. Rev. Lett. **101**, 203202 (2008).
[11] J. H. Huckans, J. R. Williams, E. L. Hazlett, R. W. Stites, and K. M. O'Hara, Phys. Rev. Lett. **102**, 165302 (2009).

[12] J. R. Williams, E. L. Hazlett, J. H. Huckans, R. W. Stites, Y. Zhang, and K. M. O'Hara, Phys. Rev. Lett. **103**, 130404 (2009).

[13] T. Lompe, T. B. Ottenstein, F. Serwane, K. Viering, A. N. Wenz, G. Zürn, and S. Jochim, Phys. Rev. Lett. **105**, 103201 (2010).

[14] R. J. Wild, P. Makotyn, P. M. Pino, E. A. Cornell, and D. S. Jin, arXiv:1112.0362.

[15] J. Wang, J. P. D'Incao, B. D. Esry, and C. H. Greene, arXiv:1201.1176.

[16] C. Chin, arXiv:1111.1484.

[17] S. Knoop, F. Ferlaino, M. Berninger, M. Mark, H.-C. Nägerl, and R. Grimm, Nature Phys. **5**, 227 (2009).

[18] S. Knoop, F. Ferlaino, M. Berninger, M. Mark, H.-C. Nägerl, and R. Grimm, J. Phys. Conf. Ser. **194**, 012064 (2009).

[19] S. Nakajima, M. Horikoshi, T. Mukaiyama, P. Naidon, and M. Ueda, Phys. Rev. Lett. **105**, 023201 (2010).

[20] S. Nakajima, M. Horikoshi, T. Mukaiyama, P. Naidon, and M. Ueda, Phys. Rev. Lett. **106**, 143201 (2011).

[21] E. Braaten and H.-W. Hammer, Ann. Phys. (Leipzig) **322**, 120 (2007).

[22] We use the correct sign before 0.97 in Eq. (1) as it appears in Ref. [21] as opposed to Ref. [1].

[23] N. Gross, Z. Shotan, O. Machtey, S. Kokkelmans, and L. Khaykovich, C.R. Physique **12**, 4 (2011).

[24] O. Machtey, Z. Shotan, N. Gross, and L. Khaykovich, arXiv:1201.2396.

[25] For the sake of simplicity we consider column density as the mean density ($\bar{n}$) multiplied by the mean path-length of the dimer through the atom cloud (l) instead of the mean column density $\overline{nl}$ [26]. The difference between the two is a constant of order 1 and will have negligible effect on the results presented here.

[26] J. Schuster, A. Marte, S. Amtage, B. Sang, G. Rempe, and H. C. W. Beijerinck, Phys. Rev. Lett. **87**, 170404 (2001).

[27] Note that the sum of all probabilities is exactly 1.

[28] D. E. Fagnan, J. Wang, C. Zhu, P. Djuricanin, B. G. Klappauf, J. L. Booth, and K. W. Madison, Phys. Rev. A **80**, 022712 (2009).

[29] This simple condition is only obtained when $v \propto 1/a$ reflecting the situation when the dimer is produced via three-body recombination with the initial kinetic energy proportional to E_d.

[30] C. Ji, D. Phillips, and L. Platter, Europhys. Lett. **92**, 13003 (2010).